nonbonded repulsions. In all other situations electronic effects should predominate and the carbonyls will adopt polyhedra that maximize the metal–carbonyl and metal–metal bonding interactions.

The calculated cluster cone angles for the $M(\eta\text{-}C_5H_5)$ fragment in clusters of the first-row transition metals suggest that an octahedral $M_6(\eta\text{-}C_5H_5)_6$ cluster is sterically saturated since there is a good match between the cluster cone angle (92°) and the ideal cone angle for an octahedron (90°), but a tetrahedral $M_4(\eta\text{-}C_5H_5)_4$ cluster is sterically unsaturated since the cluster cone angle (97°) is significantly smaller than the ideal cone angle for a tetrahedron (109.5°). Therefore, in the latter case it should be possible to incorporate additional small ligands such as CO and H into the cluster coordination sphere. These conclusions are supported by recent structural analyses on $Ni_6(\eta\text{-}C_5H_5)_6$ and $Ni_6(\eta\text{-}C_5H_5)_6^+$ by Dahl et al.[7] and the occurrence of compounds such as $Fe_4(CO)_4(\eta\text{-}C_5H_5)_4$, $Ni_4H_3(\eta\text{-}C_5H_5)_4$, and $Co_4H_4(\eta\text{-}C_5H_5)_4$.[4] The fact that the computed cone angle of $M(\eta\text{-}C_5H_5)$ is smaller than that for $M(CO)_3$ accounts for the fact that, although $Ni_6(\eta\text{-}C_5H_5)_6$ is known, the corresponding $M_6(CO)_{18}$ complexes have not been isolated for the first-row transition elements. The calculated cluster cone angles given in the table also suggest that icosahedral $M_{12}(\eta\text{-}C_5H_5)_{12}$ will be sterically very strained unless the metal–metal bond lengths greatly exceed 2.90 Å.

The development of this cluster cone-angle concept to other ligands of interest in the context of cluster chemistry, e.g., tertiary phosphines, phosphites, isocyanides, etc., is currently under investigation and will be discussed in detail in a subsequent publication. Although these computed cluster cone angles serve as a basis for a detailed discussion of cluster stoichiometries and stereochemistries, the more general qualitative point that emerges from such an analysis is that the successful synthesis of high-nuclearity clusters requires due consideration not only of the relevant electronic factors but also of the steric requirements of the ligands on the periphery of the cluster.

---

(7) Dahl, L. F.; Paquette, M. S. *J. Am. Chem. Soc.* **1980**, *102*, 6621.

Inorganic Chemistry Laboratory
University of Oxford
Oxford OX1 3QR, United Kingdom

D. M. P. Mingos

Received July 1, 1981

Structural and Theoretical Evidence for Participation of the Second Acetylene π Orbital in Transition-Metal Alkyne Complexes

Sir:

In transition-metal–olefin complexes there is no ambiguity about the role of the olefin π and π* orbitals in bonding—the classic Dewar–Chatt–Duncanson model[1,2] is a fine approximate description of what happens. An alkyne presents to a metal two π orbitals—$\pi_\perp$, **1a**, and $\pi_\parallel$, **1b**—as well as two π* orbitals, $\pi_\parallel^*$, **1c**, and $\pi_\perp^*$, **1d**. The "first" π system, $\pi_\parallel$ and $\pi_\parallel^*$, clearly acts in a manner analogous to olefin π and π*. It has been suggested that the "second" acetylene π system, $\pi_\perp$, may play an important role in bonding in some mononuclear transition-metal complexes.[3-7] There is no doubt that the $\pi_\perp$ system *can* participate in metal–alkyne interactions whenever a vacant metal d orbital of the same symmetry is present. But to what extent does it do so? Unfortunately the second π system's effect is often masked by the primary $\pi_\parallel$ and $\pi_\parallel^*$ interactions, making it difficult to isolate the $\pi_\perp$ contribution.

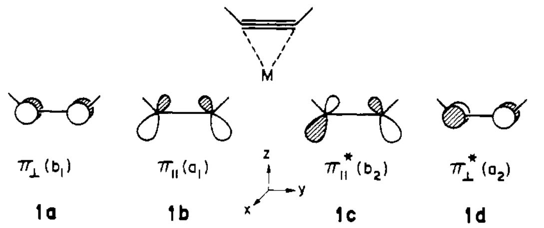

1a **1b** **1c** **1d**

Very recently structures of three diphenylacetylene complexes of Mo(II) have been determined, $(\eta^5\text{-}C_5H_5)_2Mo(PhC{\equiv}CPh)$ (**2**),[8,4c] $Mo(CN\text{-}t\text{-}Bu)_2(S\text{-}t\text{-}Bu)_2(PhC{\equiv}CPh)$ (**3**),[9] and Mo(*meso*-tetra-*p*-tolylporphyrin)(PhC≡CPh) (**4**).[4c] Although these diamagnetic molecules have the same d^4 electron count, they exhibit significant differences in the Mo–acetylene interaction. The Mo–C(acetylene) distance decreases significantly on going from **2** to **3** to **4**, while the C–C distance is slightly elongated in the same order (Table I). We wish to report here that this geometrical trend is accounted for only when the $\pi_\perp$ contribution is taken into account.

To probe the effect, we carried out extended Hückel calculations on some simplified models, $(\eta^5\text{-}C_5H_5)_2Mo(HC{\equiv}CH)$, $Mo(CNH)_2(SH)_2(HC{\equiv}CH)$, and Mo(porphyrin)(HC≡CH).[10] In each case the acetylene geometry was fixed: $h(Mo\text{-}C_2H_2) = 1.95$ Å, $r(C\text{-}C) = 1.28$ Å, $\theta(C\text{-}C\text{-}H) = 150°$. A framework for the analysis of metal–acetylene interactions is found in the conceptual construction of each complex from a metal fragment and an acetylene. We have sketched the four π orbitals of acetylene in **1a**–**d**. The frontier orbitals of each metal fragment are reasonably well-known[11] and are shown in Figure 1.

For $(\eta^5\text{-}C_5H_5)_2Mo$ the two low-lying d orbitals ($1a_1$ and b_2) and the spd-hybridized $2a_1$ lie in the *yz* plane. At higher energy there are two d orbitals (b_1 and a_2) perpendicular to the plane. An ML_4 fragment such as $Mo(CNH)_2(SH)_2$ has five frontier orbitals—three t_{2g}-like d_π orbitals (b_2, a_2, a_1) and two hybrids above them.[11b] Of those the highest hybrid combination, a_1, is omitted from Figure 1. The t_{2g} set is split substantially by the asymmetry of the ligand set—in particular a_1 is destabilized by interaction with occupied S p_π orbitals, while b_2 and a_2 are kept low by interaction with acceptor orbitals of the isocyanides. Mo(porphyrin), in which the Mo atom is moved out of the porphyrin plane by 0.63 Å, carries four low-lying d orbitals.[11c] The $x^2 - y^2$ is strongly pushed up by N lone pairs and is not shown in Figure 1.

---

(1) Dewar, M. J. S. *Bull. Soc. Chim. Fr.* **1951**, *18*, C71–79.
(2) Chatt, J.; Duncanson, L. A. *J. Chem. Soc.* **1953**, 2939–2947.
(3) (a) Ward, B. C.; Templeton, J. L. *J. Am. Chem. Soc.* **1980**, *102*, 1532–1538. (b) Templeton, J. L.; Ward, B. C. *Ibid.* **1980**, *102*, 3288–3290. (c) Templeton, J. L., to be submitted for publication.
(4) (a) Richard, L.; Weiss, R.; Newton, W. E.; Chen, G. J.-J.; McDonald, J. W. *J. Am. Chem. Soc.* **1978**, *100*, 1318–1320. (b) Newton, W. E.; McDonald, J. W.; Corbin, J. L.; Ricard, L.; Weiss, R. *Inorg. Chem.* **1980**, *19*, 1997–2006. (c) DeCian, A.; Colin, J.; Schappacher, M.; Ricard, L.; Weiss, R. *J. Am. Chem. Soc.* **1981**, *103*, 1850–1851.
(5) Cotton, F. A.; Hall, W. T. *J. Am. Chem. Soc.* **1979**, *101*, 5094–5095.
(6) King, R. B. *Inorg. Chem.* **1968**, *7*, 1044–1046.
(7) Braterman, P. S.; Davidson, J. L.; Sharp, D. W. A. *J. Chem. Soc., Dalton Trans.* **1976**, 241–245.
(8) Nakamura, A.; Otsuka, S. *J. Am. Chem. Soc.* **1972**, *94*, 1886–1894.
(9) Kamata, M.; Yoshida, T.; Otsuka, S.; Hirotsu, K.; Higuchi, T.; Kido, M.; Tatsumi, K.; Hoffmann, R. *Organometallics*, in press.
(10) Atomic parameters of Mo were taken from the literature: Kubáček, P.; Hoffmann, R. *J. Am. Chem. Soc.* **1981**, *103*, 4320–4332. The parameters for S, C, N, and H are the standard ones, and S d orbitals were excluded.
(11) (a) For Cp_2M orbitals see: Lauher, J. W.; Hoffmann, R. *J. Am. Chem. Soc.* **1976**, *98*, 1729–1742 and references therein. (b) As a leading reference for ML_4 orbitals see: Elian, M.; Hoffmann, R. *Inorg. Chem.* **1975**, *14*, 1058–1076. (c) For porphyrin orbitals see: Tatsumi, K.; Hoffmann, R. *J. Am. Chem. Soc.* **1981**, *103*, 3328–3341.

0020-1669/82/1321-0466$01.25/0

Table I. Experimental Geometry of the Three Diphenylacetylene Complexes of Mo(II)

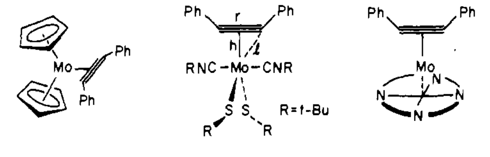

	2	3	4
r(Å)	1.269[a]	1.28[b]	1.324[a]
l(Å)	2.144	2.054	1.974
h(Å)	2.048	1.952	1.860

[a] Reference 4c. [b] Reference 9.

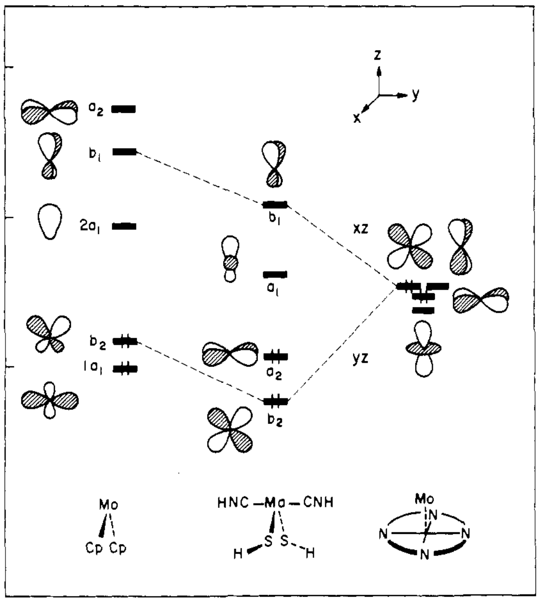

Figure 1. Frontier orbitals of Cp_2Mo, $Mo(CNH)_2(SH)_2$, and Mo(porphyrin) fragments. The energies of the important b_1 and b_2 orbitals, which will be engaged in bonding with $\pi_\perp$ and $\pi_\parallel{}^*$, respectively, are connected by dashed lines.

With the metal fragment orbitals in hand, let us consider their interaction with an acetylene. As one might expect, the basic pattern of interaction for **2**, **3**, and **4** is very much alike. A representative one may be that for **4**, Mo(porphyrin)(HC≡CH), which is given in Figure 2. Since the porphyrin orbitals are innocent of Mo–acetylene interaction, we have omitted them from the figure. The vacant acetylene $\pi_\parallel{}^*$ stabilizes strongly the metal $b_2(yz)$ orbital. Acetylene $\pi_\perp{}^*$ also pushes $a_2(xy)$ down, but only slightly. The two stabilized orbitals take care of four d electrons in the complex. The other two low-lying d orbitals are destabilized by the interactions with acetylene-occupied $\pi_\parallel$ and $\pi_\perp$ orbitals. Interestingly, $\pi_\perp$ interacts with $b_1(xz)$ just as strongly as $\pi_\parallel$ does with $a_1(z^2)$. We will come back to this point later.

All four acetylene orbitals are involved in metal–alkyne bonding. An increase in any of the four modes of interaction would lead to a strengthening of Mo–acetylene bonding. Which interaction then is responsible for the geometrical trend observed in the Mo–C and C–C bond lengths of the acetylene complexes? We think the answer is the $\pi_\perp$–$b_1(xz)$, i.e., the second π interaction. If we refer back to Figure 1, xz moves down significantly in energy going on from **2** to **3** to **4**. Since the $\pi_\perp$ energy level (−13.36 eV) is always lower than the xz level, lowering of xz enhances $\pi_\perp$–xz bonding. This is traced by our population analysis. The magnitude of electron flow from the occupied $\pi_\perp$ to the metal fragment is augmented on going from **2** to **3** to **4**: 0.147 e (**2**), 0.223 e (**3**), and 0.249 e (**4**). Thus the increase in the $\pi_\perp$–$b_1(xz)$ interaction strengthens the Mo–acetylene bond and weakens the C–C bond in the order **2** < **3** < **4**, which is in accord with the experimental observations.

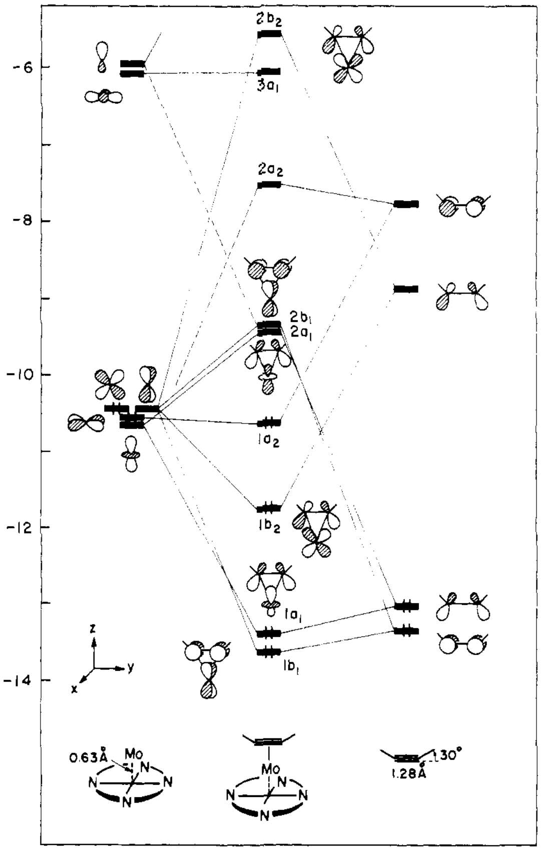

Figure 2. Interaction diagram for Mo(porphyrin) and acetylene. Minor interactions are dashed. Porphyrin π orbitals, which are innocent of Mo–acetylene interaction, are omitted from the figure.

While the observed trend is well explained by the effect of the second π system, the $\pi_\perp$–$b_1(xz)$ mixing is not the strongest one among the four types of interactions. The major interaction is between $\pi_\parallel{}^*$ and yz. A large electron flux from the metal fragments to acetylene $\pi_\parallel{}^*$ was calculated: 0.740 e (**2**), 0.584 e (**3**), and 0.803 e (**4**). The equilibrium conformation of the acetylene in the equatorial plane in **2**[12] and parallel to the trigonal-bipyramid axis in **3**[13] is set by a seeking out of the optimal $\pi_\parallel{}^*$–yz interaction, the classical back-donation, with some assistance from $\pi_\perp$–xz. Both the population analysis and the relative energy of $b_2(yz)$ of the fragments (Figure 1) indicate that the extent of $\pi_\parallel{}^*$–yz bonding increases in the order **3** < **2** < **4**. The experimentally observed Mo–C and C–C distances do not, however, follow this order. Neither do they follow the $\pi_\parallel$–a_1 nor $\pi^*{}_\perp$–a_2 electron transfers. We conclude that $\pi_\parallel{}^*$–yz and $\pi_\perp$–xz interactions are both important but play different roles in determining the detailed geometry of the acetylene complex. The $\pi_\parallel{}^*$–yz mixing sets

---

(12) The conformational preferences of the olefin equivalents of Cp_2M(alkyne) are analyzed in ref 11a.

(13) The orientation of the acetylene and SR ligands and their site preferences in **3** will be discussed by: Kamata, M.; Hirotsu, K.; Higuchi, T.; Tatsumi, K.; Hoffmann, R.; Yoshida, T.; Otsuka, S., to be submitted for publication.

(14) Two-electron donor or four-electron donor are descriptors often used or questioned in discussions of metal–alkyne bonding (ref 3–7). For example, the acetylene in **2** is regarded as a two-electron donor, while the one in **4** behaves as a four-electron donor (ref 4c). Of course, it is not meant that acetylene literally donates two or four electrons to the metal moieties. However, our calculational results are in harmony with the spirit of this handy criterion, at least for **2** and **4**. In **4**, electron donation from the acetylene $\pi_\perp$ (0.249 e) amounts to as much as that from $\pi_\parallel$ (0.225 e). The interaction diagram of Figure 2 is supportive of the population analysis, since the $\pi_\perp$–$b_1(xz)$ and $\pi_\parallel$–$a_1(z^2)$ interactions are roughly equivalent in magnitude. For **2**, on the other hand, donation from $\pi_\perp$ (0.147 e) is much less than that from $\pi_\parallel$ (0.228 e).

the equilibrium geometry (e.g., in **2** or **3**) but the $\pi_{\perp}$–xz interaction is indispensable—it fine tunes the metal–acetylene bonding.[14]

Acknowledgment. We are grateful to S. Otsuka and R. Weiss for communication of structural data prior to publication. Our research was supported by the National Science Foundation through Research Grant CHE 7828048. J.L.T. thanks the donors of the Petroleum Research Fund, administered by the American Chemical Society, for support of this work.

Registry No. **2**, 12701-46-1; **3**, 79681-75-7; **4**, 79681-76-8.

Department of Chemistry
Cornell University
Ithaca, New York 14853
Kazuyuki Tatsumi
Roald Hoffmann*

Department of Chemistry
The University of North Carolina
Chapel Hill, North Carolina 27514
Joseph L. Templeton

Received September 8, 1981